加权融合鲁棒增量Kalman滤波器

孙小君①② 周 晗*① 沈海滨① 闫广明①②
①(黑龙江大学电子工程学院 哈尔滨 150080)
②(黑龙江省信息融合估计与检测重点实验室 哈尔滨 150080)

摘 要：在一定环境条件下，当系统的量测方程没有进行验证或校准时，使用该量测方程往往会产生未知的系统误差，从而导致较大的滤波误差。同样地，当系统的噪声方差不确定时，滤波的性能也将会变坏，甚至会引起滤波器发散。增量方程的引入可以有效消除系统的未知量测误差，从而带未知量测误差的欠观测系统的状态估计问题可以转换为增量系统的状态估计问题。该文考虑带未知量测误差和未知噪声方差的线性离散系统，首先提出一种基于增量方程的鲁棒增量Kalman滤波器。进而，基于线性最小方差最优融合准则，提出一种加权融合鲁棒增量Kalman滤波算法。仿真实例证明了所提算法的有效性和可行性。

关键词：信息融合；加权融合；欠观测系统；增量滤波；鲁棒性
中图分类号：TN713, TP18 **文献标识码**：A **文章编号**：1009-5896(2021)12-3680-07
DOI: 10.11999/JEIT200122

Weighted Fusion Robust Incremental Kalman Filter

SUN Xiaojun①② ZHOU Han① SHEN Haibin① YAN Guangming①②
①(*Electrical Engineering Institute, Heilongjiang University, Harbin* 150080, *China*)
②(*Key Laboratory of Information Fusion Estimation and Detection, Heilongjiang Province, Harbin* 150080, *China*)

Abstract: Under certain environmental conditions, when the measurement equation of the system is not verified or calibrated, the use of the measurement equation will often produce unknown system errors, resulting in large filtering errors. Similarly, when the noise variance of the system is uncertain, the performance of the filter will deteriorate, and even cause the filter divergence. The introduction of incremental equation can effectively eliminate the unknown measurement error of the system, so that the state estimation of system under poor observation condition with unknown measurement error can be transformed into the state estimation of incremental system. In this paper, a robust incremental Kalman filter based on incremental equation is proposed for linear discrete systems with unknown measurement error and unknown noise variance. Then, based on the linear minimum variance optimal fusion criterion, a weighted fusion robust incremental Kalman filtering algorithm is proposed. Simulation results show the effectiveness and feasibility of the proposed algorithm.

Key words: Information fusion; Weighted fusion; Systems under poor observation condition; Incremental filtering; Robustness

1 引言

Kalman滤波是Kalman于1960年提出的一种重要的状态估计方法[1,2]。这种最优递推滤波算法克服了经典Wiener滤波理论的缺点和局限性，便于在计算机上递推实现，计算量和存储量小，适合处理非平稳随机信号或时变随机系统的滤波问题[3,4]。目前广泛地应用于制导、全球定位系统、组合导航、目标跟踪、故障诊断、图像处理等领域[5–7]。

然而，Kalman滤波算法的局限性是要求精确已知系统模型参数和噪声统计[8]。在许多实际应用问题中，由于周围环境的影响、测量设备自身造成的误差、模型和参数选取不当等，会产生量测系统

收稿日期：2020-02-21；改回日期：2021-03-07；网络出版：2021-03-29
*通信作者： 周晗 1120546259@qq.com
基金项目：国家自然科学基金(61104209)，黑龙江省高校基本科研业务费黑龙江大学专项资金(2020-KYYWF-0998)
Foundation Items: The National Natural Science Foundation of China (61104209), The Special Funds of Heilongjiang University of Basic Scientific Research Expenses for Colleges and Universities in Heilongjiang Province (2020-KYYWF-0998)

误差，而使用传统Kalman滤波算法难以消除该类系统的误差[9]。目前针对这个问题，已有一系列增量滤波算法被提出。文献[10,11]针对欠观测的非线性系统，分别提出了扩展增量Kalman滤波算法和增量粒子滤波算法。文献[12–14]针对欠观测的线性系统，分别提出了增量Kalman滤波算法、自适应增量滤波算法和加权观测融合增量滤波算法。它们都通过引入增量观测方程成功地消除了系统的未知量测误差，提高了欠观测系统状态估计的精度。关于增量滤波的应用研究，近年来也不断涌现：文献[15]将增量卡尔曼滤波算法应用到室内超宽带(Ultra WideBand，UWB)定位算法中以消除非视距(Non-Line-Of-Sight，NLOS)误差和卡尔曼滤波中由量测方程带来的量测系统误差。文献[16]基于增量Kalman滤波方法对于全球定位系统(Global Positioning System, GPS)多路径效应系统误差进行研究。文献[17]提出一种基于增量式卡尔曼滤波器的转子转速滤波算法，用来滤除永磁同步电机转子转速测量环节存在的量化误差等噪声。

当系统的噪声方差不确定时，Kalman滤波器的性能同样也将变坏，甚至引起滤波器发散[18]。为了克服这个局限性，鲁棒Kalman滤波的研究也备受人们关注。目前，许多鲁棒Kalman滤波的文献主要考虑模型参数不确定性的系统，而噪声方差被假定是精确已知的。文献[19,20]分别提出了有限视野(时变)鲁棒Kalman滤波器和无限视野(稳态)鲁棒Kalman滤波器。但他们仅考虑了模型参数的不确定性而噪声方差被假设为精确已知。对于带噪声方差不确定性的不确定系统，鲁棒Kalman滤波器的报道较少[21–23]。对于带单传感器和不确定噪声方差的广义系统和2维系统，相应的鲁棒Kalman滤波器分别被提出[21,22]。对于带不确定参数和噪声方差的单传感器系统，用Riccati方程方法，一种鲁棒Kalman滤波器被提出[23]。但对于带未知量测系统误差和未知噪声方差的不确定系统的鲁棒增量Kalman滤波算法问题尚无相关研究。

针对现有多传感器不确定系统的信息融合滤波理论的上述局限性和问题，本文将首先针对带未知量测系统误差和未知噪声方差的单传感器不确定系统提出一种基于增量方程的鲁棒增量Kalman滤波算法。进而提出一种最优加权观测融合鲁棒增量Kalman滤波算法。并分别进行了鲁棒性分析。仿真实验验证了所提出的算法的有效性。

2　问题描述

考虑带不确定噪声方差的多传感器线性离散时变欠观测系统的状态方程

$$\boldsymbol{x}_k = \boldsymbol{\Phi}_{k-1}\boldsymbol{x}_{k-1} + \boldsymbol{\Gamma}_{k-1}\boldsymbol{w}_{k-1} \tag{1}$$

增量观测方程为

$$\Delta \boldsymbol{z}_k^{(i)} = \boldsymbol{H}_k^{(i)} x_k - \boldsymbol{H}_{k-1}^{(i)}\boldsymbol{x}_{k-1} + \boldsymbol{V}_k^{(i)} \tag{2}$$

其中，k为离散时间，系统在k时刻的状态为$\boldsymbol{x}_k \in \boldsymbol{R}^n$，$\boldsymbol{\Phi}_{k-1} \in \boldsymbol{R}^{n\times n}$为状态转移矩阵。$\Delta\boldsymbol{z}_k^{(i)}$表示第$i$个子系统在$k$时刻的观测值增量，$\Delta\boldsymbol{z}_k^{(i)} = \boldsymbol{z}_k^{(i)} - \boldsymbol{z}_{k-1}^{(i)}$，$\boldsymbol{H}_k^{(i)} \in \boldsymbol{R}^{m\times n}$为第$i$个子系统在$k$时刻的观测矩阵。

假设1　$\boldsymbol{w}_k \in \boldsymbol{R}^r$和$\boldsymbol{V}_k^{(i)}$是带零均值、实际方差分别为$\bar{\boldsymbol{Q}}_k$和$\bar{\boldsymbol{R}}_k^{(i)}$的不相关白噪声，但$\bar{\boldsymbol{Q}}_k$和$\bar{\boldsymbol{R}}_k^{(i)}$是未知不确定的，仅已知它们的上界$\boldsymbol{Q}_k$和$\boldsymbol{R}_k^{(i)}$，即

$$\bar{\boldsymbol{Q}}_k \le \boldsymbol{Q}_k, \bar{\boldsymbol{R}}_k^{(i)} \le \boldsymbol{R}_k^{(i)}, i = 1, 2, \cdots, L, \forall k \tag{3}$$

并且

$$\mathrm{E}\left\{\begin{bmatrix} w_k \\ \boldsymbol{V}_k^{(i)} \end{bmatrix}\begin{bmatrix} w_l^{\mathrm{T}} & \boldsymbol{V}_l^{(j)\mathrm{T}} \end{bmatrix}\right\} = \begin{bmatrix} \bar{\boldsymbol{Q}}_k & 0 \\ 0 & \bar{\boldsymbol{R}}_k^{(i)}\delta_{ij} \end{bmatrix}\delta_{kl} \tag{4}$$

其中，E是数学期望算子，T为转置算子，δ_{ij}为Kronecker函数，$\delta_{ii} = 1$，$\delta_{ij} = 0(i \ne j)$。

假设2　初始状态$\boldsymbol{x}_0$与白噪声$\boldsymbol{w}_k$和$\boldsymbol{V}_k^{(i)}$不相关，带均值为μ和未知不确定实际方差阵$\bar{\boldsymbol{P}}_{0|0}$，且满足

$$\bar{\boldsymbol{P}}_{0|0} \le \boldsymbol{P}_{0|0} \tag{5}$$

其中，$\boldsymbol{P}_{0|0}$是$\bar{\boldsymbol{P}}_{0|0}$的已知保守上界。

注1 对隐含的多源量测系统误差，因工程实际中，相邻两个量测$\boldsymbol{z}_k^{(i)}$和$\boldsymbol{z}_{k-1}^{(i)}$的测量系统误差大小比较接近，所以$\Delta\boldsymbol{z}_k^{(i)}$的系统误差为相对小量，可以忽略不计[9]。当然，所得到的增量滤波的精度是会低于量测误差精确已知时的情况。但在量测误差未知的情况下，这种方法比“自校准”更简单[9]，比直接应用经典Kalman滤波的精度也要高得多[12]。并且，由独立增量随机过程原理可知，$\Delta\boldsymbol{z}_k^{(i)}$与$\Delta\boldsymbol{z}_{k-1}^{(i)}$之间比$\boldsymbol{z}_k^{(i)}$与$\boldsymbol{z}_{k-1}^{(i)}$更能满足假设1的独立性要求[24]。

问题是对带不确定噪声方差的不确定增量系统式(1)和式(2)设计一个局部和加权融合鲁棒增量Kalman滤波器$\hat{\boldsymbol{x}}_{k|k}^{(i)}$和$\hat{\boldsymbol{x}}_{k|k}^{(w)}$，对所有容许的满足式(3)和式(5)的不确定噪声方差$\bar{\boldsymbol{Q}}_k$, $\bar{\boldsymbol{R}}_k^{(i)}$和不确定初值$\bar{\boldsymbol{P}}_{0|0}$，使它的相应的实际滤波误差方差阵$\bar{\boldsymbol{P}}_{k|k}^{(i)}$保证有一个最小上界$\boldsymbol{P}_{k|k}^{(i)}$[2]，即满足

$$\bar{\boldsymbol{P}}_{k|k}^{(i)} \le \boldsymbol{P}_{k|k}^{(i)} \tag{6}$$

3 局部鲁棒增量Kalman滤波器

定理1 带保守上界噪声方差$\boldsymbol{Q}_k$和$\boldsymbol{R}_k^{(i)}$的最坏情形的保守系统式(1)和系统式(2)在假设1和假设2下，有局部保守最优增量Kalman滤波器为

$$\hat{\boldsymbol{x}}_{k|k-1}^{(i)}=\boldsymbol{\Phi}_{k-1}\hat{\boldsymbol{x}}_{k-1|k-1}^{(i)} \tag{7}$$

$$\boldsymbol{P}_{k|k-1}^{(i)}=\boldsymbol{\Phi}_{k-1}\boldsymbol{P}_{k-1|k-1}^{(i)}\boldsymbol{\Phi}_{k-1}^{\mathrm{T}}+\boldsymbol{\Gamma}_{k-1}\boldsymbol{Q}_{k-1}\boldsymbol{\Gamma}_{k-1}^{\mathrm{T}} \tag{8}$$

$$\hat{\boldsymbol{x}}_{k|k}^{(i)}=\hat{\boldsymbol{x}}_{k|k-1}^{(i)}+\boldsymbol{K}_k^{f(i)}(\Delta\boldsymbol{z}_k^{(i)}-\Delta\hat{\boldsymbol{z}}_{k|k-1}^{(i)}) \tag{9}$$

$$\boldsymbol{P}_{k|k}^{(i)}=\boldsymbol{P}_{k|k-1}^{(i)}-\boldsymbol{K}_k^{f(i)}\boldsymbol{\Omega}_k^{(i)}\boldsymbol{K}_k^{f(i)\mathrm{T}} \tag{10}$$

$$\boldsymbol{K}_k^{f(i)}=(\boldsymbol{P}_{k|k-1}^{(i)}\boldsymbol{H}_k^{(i)\mathrm{T}}-\boldsymbol{\Phi}_{k-1}\boldsymbol{P}_{k-1|k-1}^{(i)}\boldsymbol{H}_{k-1}^{(i)\mathrm{T}})\boldsymbol{\Omega}_k^{(i)-1} \tag{11}$$

$$\Delta\hat{\boldsymbol{z}}_{k|k-1}^{(i)}=\boldsymbol{H}_k^{(i)}\hat{\boldsymbol{x}}_{k|k-1}^{(i)}-\boldsymbol{H}_{k-1}^{(i)}\hat{\boldsymbol{x}}_{k-1|k-1}^{(i)} \tag{12}$$

$$\begin{aligned}\boldsymbol{\Omega}_k^{(i)}=&\boldsymbol{H}_k^{(i)}\boldsymbol{P}_{k|k-1}^{(i)}\boldsymbol{H}_k^{(i)\mathrm{T}}+\boldsymbol{R}_k^{(i)}-\boldsymbol{H}_{k-1}^{(i)}\boldsymbol{P}_{k-1|k-1}^{(i)}\\&\cdot\boldsymbol{\Phi}_{k-1}^{\mathrm{T}}\boldsymbol{H}_k^{(i)\mathrm{T}}-\boldsymbol{H}_k^{(i)}\boldsymbol{\Phi}_{k-1}\boldsymbol{P}_{k-1|k-1}^{(i)}\boldsymbol{H}_{k-1}^{(i)\mathrm{T}}\\&+\boldsymbol{H}_{k-1}^{(i)}\boldsymbol{P}_{k-1|k-1}^{(i)}\boldsymbol{H}_{k-1}^{(i)\mathrm{T}}\end{aligned} \tag{13}$$

证明 由文献[12]的单传感器增量Kalman滤波器，易得定理1。

注2 带时变增益$\boldsymbol{K}_k^{f(i)}$的保守Kalman滤波器，式(7)为时变Kalman滤波器，其中，由带保守上界方差的保守系统式(1)和系统式(2)生成的保守观测是不可利用的。只有由带实际噪声方差的系统式(1)和式(2)生成的观测是可利用的，它可通过传感器观测得到。因此，在式(7)中用实际观测代替保守观测就得到实际局部增量Kalman滤波器。

代入实际噪声方差易得

$$\bar{\boldsymbol{P}}_{k|k-1}^{(i)}=\boldsymbol{\Phi}_{k-1}\bar{\boldsymbol{P}}_{k-1|k-1}^{(i)}\boldsymbol{\Phi}_{k-1}^{\mathrm{T}}+\boldsymbol{\Gamma}_{k-1}\bar{\boldsymbol{Q}}_{k-1}\boldsymbol{\Gamma}_{k-1}^{\mathrm{T}} \tag{14}$$

$$\bar{\boldsymbol{P}}_{k|k}^{(i)}=\bar{\boldsymbol{P}}_{k|k-1}^{(i)}-\bar{\boldsymbol{K}}_k^{f(i)}\boldsymbol{\Omega}_k^{(i)}\bar{\boldsymbol{K}}_k^{f(i)\mathrm{T}} \tag{15}$$

$$\bar{\boldsymbol{K}}_k^{f(i)}=(\bar{\boldsymbol{P}}_{k|k-1}^{(i)}\boldsymbol{H}_k^{(i)\mathrm{T}}-\boldsymbol{\Phi}_{k-1}\bar{\boldsymbol{P}}_{k-1|k-1}^{(i)}\boldsymbol{H}_{k-1}^{(i)\mathrm{T}})\bar{\boldsymbol{\Omega}}_k^{(i)-1} \tag{16}$$

$$\begin{aligned}\bar{\boldsymbol{\Omega}}_k^{(i)}=&\boldsymbol{H}_k^{(i)}\bar{\boldsymbol{P}}_{k|k-1}^{(i)}\boldsymbol{H}_k^{(i)\mathrm{T}}+\bar{\boldsymbol{R}}_k^{(i)}-\boldsymbol{H}_{k-1}^{(i)}\bar{\boldsymbol{P}}_{k-1|k-1}^{(i)}\\&\cdot\boldsymbol{\Phi}_{k-1}^{\mathrm{T}}\boldsymbol{H}_k^{(i)\mathrm{T}}-\boldsymbol{H}_k^{(i)}\boldsymbol{\Phi}_{k-1}\bar{\boldsymbol{P}}_{k-1|k-1}^{(i)}\boldsymbol{H}_{k-1}^{(i)\mathrm{T}}\\&+\boldsymbol{H}_{k-1}^{(i)}\bar{\boldsymbol{P}}_{k-1|k-1}^{(i)}\boldsymbol{H}_{k-1}^{(i)\mathrm{T}}\end{aligned} \tag{17}$$

定理2 多传感器不确定系统式(1)和式(2)在假设1和假设2下，带保守上界方差$\boldsymbol{Q}_k$和$\boldsymbol{R}_k^{(i)}$和初值$\boldsymbol{P}_{0|0}$的实际局部Kalman滤波器是鲁棒的，即对所有容许的满足式(3)的$\bar{\boldsymbol{Q}}_k$, $\bar{\boldsymbol{R}}_k^{(i)}$和满足式(5)的初值$\bar{\boldsymbol{P}}_{0|0}$，相应的由式(15)给出的实际滤波误差方差阵$\bar{\boldsymbol{P}}_{k|k}^{(i)}$满足

$$\bar{\boldsymbol{P}}_{k|k}^{(i)}\le\boldsymbol{P}_{k|k}^{(i)} \tag{18}$$

其中，保守滤波误差方差阵$\boldsymbol{P}_{k|k}^{(i)}$由式(10)给出，且$\boldsymbol{P}_{k|k}^{(i)}$是$\bar{\boldsymbol{P}}_{k|k}^{(i)}$的最小上界。由此称局部增量Kalman滤波器为局部鲁棒增量Kalman滤波器。

证明 由式(1)和式(7)得

$$\tilde{\boldsymbol{x}}_{k|k-1}^{(i)}=\boldsymbol{x}_k-\hat{\boldsymbol{x}}_{k|k-1}^{(i)}=\boldsymbol{\Phi}_{k-1}\tilde{\boldsymbol{x}}_{k-1|k-1}^{(i)}+\boldsymbol{\Gamma}_{k-1}w_{k-1} \tag{19}$$

进而由式(9)有

$$\tilde{\boldsymbol{x}}_{k|k}^{(i)}=\boldsymbol{x}_k-\hat{\boldsymbol{x}}_{k|k}^{(i)}=\tilde{\boldsymbol{x}}_{k|k-1}^{(i)}-\boldsymbol{K}_k^{f(i)}(\Delta\boldsymbol{z}_k^{(i)}-\Delta\hat{\boldsymbol{z}}_{k|k-1}^{(i)}) \tag{20}$$

代入式(12)，又由式(2)可得

$$\begin{aligned}\tilde{\boldsymbol{x}}_{k|k}^{(i)}=&x_k-\hat{\boldsymbol{x}}_{k|k}^{(i)}=\tilde{\boldsymbol{x}}_{k|k-1}^{(i)}-\boldsymbol{K}_k^{f(i)}\\&\cdot(\boldsymbol{H}_k^{(i)}\tilde{\boldsymbol{x}}_{k|k-1}^{(i)}-\boldsymbol{H}_{k-1}^{(i)}\tilde{\boldsymbol{x}}_{k-1|k-1}^{(i)}+V_k^{(i)})\\=&[\boldsymbol{I}_n-\boldsymbol{K}_k^{f(i)}\boldsymbol{H}_k^{(i)}]\tilde{\boldsymbol{x}}_{k|k-1}^{(i)}\\&+\boldsymbol{K}_k^{f(i)}\boldsymbol{H}_{k-1}^{(i)}\tilde{\boldsymbol{x}}_{k-1|k-1}^{(i)}-\boldsymbol{K}_k^{f(i)}V_k^{(i)}\end{aligned} \tag{21}$$

代入式(19)得

$$\begin{aligned}\tilde{\boldsymbol{x}}_{k|k}^{(i)}=&[\boldsymbol{I}_n-\boldsymbol{K}_k^{f(i)}\boldsymbol{H}_k^{(i)}][\boldsymbol{\Phi}_{k-1}\tilde{\boldsymbol{x}}_{k-1|k-1}^{(i)}+\boldsymbol{\Gamma}_{k-1}w_{k-1}]\\&+\boldsymbol{K}_k^{f(i)}\boldsymbol{H}_{k-1}^{(i)}\tilde{\boldsymbol{x}}_{k-1|k-1}^{(i)}-\boldsymbol{K}_k^{f(i)}V_k^{(i)}\\=&[(\boldsymbol{I}_n-\boldsymbol{K}_k^{f(i)}\boldsymbol{H}_k^{(i)})\boldsymbol{\Phi}_{k-1}+\boldsymbol{K}_k^{f(i)}\boldsymbol{H}_{k-1}^{(i)}]\tilde{\boldsymbol{x}}_{k-1|k-1}^{(i)}\\&+(I_n-\boldsymbol{K}_k^{f(i)}\boldsymbol{H}_k^{(i)})\boldsymbol{\Gamma}_{k-1}w_{k-1}-\boldsymbol{K}_k^{f(i)}V_k^{(i)}\\=&\boldsymbol{\Psi}_k^{(i)}\tilde{\boldsymbol{x}}_{k-1|k-1}^{(i)}+(\boldsymbol{I}_n-\boldsymbol{K}_k^{f(i)}\boldsymbol{H}_k^{(i)})\boldsymbol{\Gamma}_{k-1}w_{k-1}\\&-\boldsymbol{K}_k^{f(i)}V_k^{(i)}\end{aligned} \tag{22}$$

其中，$\boldsymbol{\Psi}_k^{(i)}=(\boldsymbol{I}_n-\boldsymbol{K}_k^{f(i)}\boldsymbol{H}_k^{(i)})\boldsymbol{\Phi}_{k-1}+\boldsymbol{K}_k^{f(i)}\boldsymbol{H}_{k-1}^{(i)}$。

由式(22)，根据假设1和假设2，注意到$\boldsymbol{w}_k$，$\boldsymbol{V}_k^{(i)}$和$\tilde{\boldsymbol{x}}_{k-1|k-1}^{(i)}$不相关，所以实际滤波误差方差阵

$$\begin{aligned}\bar{\boldsymbol{P}}_{k|k}^{(i)}=&\boldsymbol{\Psi}_k^{(i)}\bar{\boldsymbol{P}}_{k-1|k-1}^{(i)}\boldsymbol{\Psi}_k^{(i)\mathrm{T}}+(\boldsymbol{I}_n-\boldsymbol{K}_k^{f(i)}\boldsymbol{H}_k^{(i)})\boldsymbol{\Gamma}_{k-1}\\&\cdot\bar{\boldsymbol{Q}}_{k-1}\boldsymbol{\Gamma}_{k-1}^{\mathrm{T}}(\boldsymbol{I}_n-\boldsymbol{K}_k^{f(i)}\boldsymbol{H}_k^{(i)})^{\mathrm{T}}\\&+\boldsymbol{K}_k^{f(i)}\bar{\boldsymbol{R}}_k^{(i)}\boldsymbol{K}_k^{f(i)\mathrm{T}}\end{aligned} \tag{23}$$

定义$\Delta_{k|k}^{(i)}=\boldsymbol{P}_{k|k}^{(i)}-\bar{\boldsymbol{P}}_{k|k}^{(i)}$，由式(23)的Lyapunov方程

$$\Delta_{k|k}^{(i)}=\boldsymbol{\Psi}_k^{(i)}\Delta_{k-1|k-1}^{(i)}\boldsymbol{\Psi}_k^{(i)\mathrm{T}}+U_k^{(i)} \tag{24}$$

$$\begin{aligned}\boldsymbol{U}_k^{(i)}=&(\boldsymbol{I}_n-\boldsymbol{K}_k^{f(i)}\boldsymbol{H}_k^{(i)})\boldsymbol{\Gamma}_{k-1}(\boldsymbol{Q}_{k-1}-\bar{\boldsymbol{Q}}_{k-1})\boldsymbol{\Gamma}_{k-1}^{\mathrm{T}}\\&\cdot(\boldsymbol{I}_n-\boldsymbol{K}_k^{f(i)}\boldsymbol{H}_k^{(i)})^{\mathrm{T}}+\boldsymbol{K}_k^{f(i)}(\boldsymbol{R}_k^{(i)}-\bar{\boldsymbol{R}}_k^{(i)})\boldsymbol{K}_k^{f(i)\mathrm{T}}\end{aligned} \tag{25}$$

应用式(3)和式(25)得$\boldsymbol{U}_k^{(i)}\ge 0$，由式(5)有$\boldsymbol{\Delta}_{0|0}^{(i)}=\boldsymbol{P}_{0|0}^{(i)}-\bar{\boldsymbol{P}}_{0|0}^{(i)}\ge 0$。因此由式(24)得$\boldsymbol{\Delta}_{1|1}^{(i)}\ge 0$。应用数学归纳法对所有时刻$k$有$\boldsymbol{\Delta}_{k|k}^{(i)}\ge 0$，即不等式(18)成立。取$\bar{\boldsymbol{Q}}_k^{(i)}=\boldsymbol{Q}_k^{(i)}$ ，$\bar{\boldsymbol{R}}_k^{(i)}=\boldsymbol{R}_k^{(i)}$和$\bar{\boldsymbol{P}}_{0|0}^{(i)}=$

$P_{0|0}^{(i)}$，约束条件式(3)和式(5)成立，且对任意$k\ge 0$有$\boldsymbol{U}_k^{(i)}=0$，并且$\boldsymbol{\Delta}_{0|0}^{(i)}=0$，进而由式(24)得$\boldsymbol{\Delta}_{1|1}^{(i)}=0$，且用数学归纳法递推可得$\boldsymbol{\Delta}_{k|k}^{(i)}=0$, $k\ge 1$。这引出$\bar{\boldsymbol{P}}_{k|k}^{(i)}=P_{k|k}^{(i)}$, $k\ge 0$。对任意另一个上界$\bar{\boldsymbol{P}}_{k|k}^{*(i)}$，得$\boldsymbol{P}_{k|k}^{(i)}=\bar{\boldsymbol{P}}_{k|k}^{(i)}\le\bar{\boldsymbol{P}}_{k|k}^{*(i)}$，引出$\boldsymbol{P}_{k|k}^{(i)}$是实际误差方差阵$\bar{\boldsymbol{P}}_{k|k}^{(i)}$的最小上界误差方差阵。　证毕

注3 鲁棒性即为“稳健性”，是指在外界容许的不确定干扰下仍能保证实现预期性能指标。对带真实噪声方差阵$\bar{\boldsymbol{Q}}_k^{(i)}=\boldsymbol{Q}_k^{(i)}$，$\bar{\boldsymbol{R}}_k^{(i)}=\boldsymbol{R}_k^{(i)}$的实际系统式(1)和式(2)，可得相应的实际滤波误差方差阵$\bar{\boldsymbol{P}}_{k|k}^{(i)}$。对于每一对满足约束式(3)的$(\bar{\boldsymbol{Q}}_k,\ \bar{\boldsymbol{R}}_k^{(i)})$，均可以得到相应的一个实际的误差方差阵。因而对所有容许的满足约束式(3)的$(\bar{\boldsymbol{Q}}_k,\ \bar{\boldsymbol{R}}_k^{(i)})$，得到一簇系统式(1)和式(2)以及相应容许的实际误差方差阵$\bar{\boldsymbol{P}}_{k|k}^{(i)}$的一个集合$\mathcal{P}_i$。定理2根据Kalman滤波器的性质，基于Lyapunov方程证明了由不等式(3)可引出对所有容许的$\bar{\boldsymbol{P}}_{k|k}^{(i)}\in\mathcal{P}_i$，不等式(18)成立，且可证明$\bar{\boldsymbol{P}}_{k|k}^{(i)}$是$\bar{\boldsymbol{P}}_{k|k}^{(i)}\in\mathcal{P}_i$的最小上界，因而实现了式(18)意义上的鲁棒滤波器的设计。

4　加权融合鲁棒增量Kalman滤波器

由式(2)有

$$\begin{aligned}\Delta\boldsymbol{z}_k^{(i)}&=\boldsymbol{H}_k^{(i)}x_k-\boldsymbol{H}_{k-1}^{(i)}x_{k-1}+\boldsymbol{V}_k^{(i)}\\&=\tilde{\boldsymbol{H}}_k^{(i)}x_{k-1}+\tilde{\boldsymbol{V}}_k^{(i)},\ i=1,2,\cdots,L\end{aligned}\tag{26}$$

$$\tilde{\boldsymbol{H}}_k^{(i)}=\boldsymbol{H}_k^{(i)}\boldsymbol{\Phi}_{k-1}-\boldsymbol{H}_{k-1}^{(i)}\tag{27}$$

$$\tilde{\boldsymbol{V}}_k^{(i)}=\boldsymbol{H}_k^{(i)}\boldsymbol{\Gamma}_{k-1}\boldsymbol{w}_{k-1}+\boldsymbol{V}_k^{(i)}\tag{28}$$

引入保守集中式融合观测方程

$$\Delta z_k^{(c)}=\tilde{\boldsymbol{H}}_k^{(c)}\boldsymbol{x}_{k-1}+\tilde{\boldsymbol{V}}_k^{(c)}\tag{29}$$

其中，定义

$$\left.\begin{aligned}\Delta\boldsymbol{z}_k^{(c)}&=\left[\Delta\boldsymbol{z}_k^{(1)},\Delta\boldsymbol{z}_k^{(2)},\cdots,\Delta\boldsymbol{z}_k^{(L)}\right]^{\mathrm{T}}\\\tilde{\boldsymbol{H}}_k^{(c)}&=\left[\tilde{\boldsymbol{H}}_k^{(1)},\tilde{\boldsymbol{H}}_k^{(2)},\cdots,\tilde{\boldsymbol{H}}_k^{(L)}\right]^{\mathrm{T}}\\\tilde{\boldsymbol{V}}_k^{(c)}&=\left[\tilde{\boldsymbol{V}}_k^{(1)},\tilde{\boldsymbol{V}}_k^{(2)},\cdots,\tilde{\boldsymbol{V}}_k^{(L)}\right]^{\mathrm{T}}\end{aligned}\right\}\tag{30}$$

从而可得融合观测噪声的方差阵为

$$\tilde{\boldsymbol{R}}_k^{(c)}=\mathrm{diag}(\tilde{\boldsymbol{R}}_k^{(1)},\tilde{\boldsymbol{R}}_k^{(2)},\cdots,\tilde{\boldsymbol{R}}_k^{(L)})\tag{31}$$

由式(28)可见$\boldsymbol{w}_{k-1}$和$\tilde{\boldsymbol{V}}_k^{(c)}$是相关的，且有互协方差阵为

$$\tilde{\boldsymbol{S}}_k^{(c)}=\mathrm{E}[\boldsymbol{w}_{k-1}\tilde{\boldsymbol{V}}_k^{(c)\mathrm{T}}]=\left[\tilde{\boldsymbol{S}}_k^{(i)},\cdots,\tilde{\boldsymbol{S}}_k^{(i)}\right]\tag{32}$$

其中，$\tilde{\boldsymbol{S}}_k^{(i)}=\boldsymbol{Q}_{k-1}\boldsymbol{\Gamma}_{k-1}^{\mathrm{T}}\boldsymbol{H}_k^{(i)\mathrm{T}}$。

带保守上界噪声方差$\boldsymbol{Q}_k$和$\boldsymbol{R}_k^{(i)}$的最坏情形的保守系统式(1)和式(2)在假设1和假设2下，应用增量Kalman滤波式(7)—式(13)，带保守和实际滤波误差方差阵$\boldsymbol{P}_{k|k}^{(c)}$和$\bar{\boldsymbol{P}}_{k|k}^{(c)}$的集中式融合鲁棒增量Kalman滤波器可由类似于式(7)—式(13)的公式计算得到，类似可证明鲁棒性关系

$$\bar{\boldsymbol{P}}_{k|k}^{(c)}\le\boldsymbol{P}_{k|k}^{(c)}\tag{33}$$

其中，$\boldsymbol{P}_{k|k}^{(c)}$是实际误差方差阵$\bar{\boldsymbol{P}}_{k|k}^{(c)}$的最小上界。

当$\boldsymbol{H}_k^{(i)}=H_k$即局部传感器具有相同的观测阵时，$\tilde{\boldsymbol{H}}_k=\boldsymbol{H}_k\boldsymbol{\Phi}_{k-1}-\boldsymbol{H}_{k-1}$，式(29)可以看成是对$\tilde{\boldsymbol{H}}_k\boldsymbol{x}_{k-1}$的观测矩阵[2]，从而有合成的观测模型

$$\Delta\boldsymbol{z}_k^{(c)}=\boldsymbol{e}\tilde{\boldsymbol{H}}_kx_{k-1}+\tilde{\boldsymbol{V}}_k^{(c)}\tag{34}$$

其中，$\boldsymbol{e}^{\mathrm{T}}=[I_r,I_r,\cdots,I_r]$。从而应用加权最小二乘法(Weighted Least Square, WLS)有关于$\tilde{\boldsymbol{H}}_k\boldsymbol{x}_{k-1}$的Gauss-Markov估值器

$$\Delta\boldsymbol{z}_k^{(w)}=\left[\boldsymbol{e}^{\mathrm{T}}\tilde{\boldsymbol{R}}_k^{(c)-1}\boldsymbol{e}\right]^{-1}\boldsymbol{e}^{\mathrm{T}}\tilde{\boldsymbol{R}}_k^{(c)-1}\Delta\boldsymbol{z}_k^{(c)}\tag{35}$$

且有加权融合方程

$$\Delta\boldsymbol{z}_k^{(w)}=\tilde{\boldsymbol{H}}_k\boldsymbol{x}_{k-1}+\tilde{\boldsymbol{V}}_k^{(w)}\tag{36}$$

其中，$\tilde{\boldsymbol{V}}_k^{(w)}$是对$\tilde{H}_k\boldsymbol{x}_{k-1}$的观测误差。将式(34)代入式(35)引出式(36)，且有

$$\tilde{\boldsymbol{V}}_k^{(w)}=\left[\boldsymbol{e}^{\mathrm{T}}\tilde{\boldsymbol{R}}_k^{(c)-1}\boldsymbol{e}\right]^{-1}\boldsymbol{e}^{\mathrm{T}}\tilde{\boldsymbol{R}}_k^{(c)-1}\tilde{\boldsymbol{V}}_k^{(c)}\tag{37}$$

这是带零均值的白噪声，其方差为

$$\tilde{\boldsymbol{R}}_k^{(w)}=\left[\boldsymbol{e}^{\mathrm{T}}\tilde{\boldsymbol{R}}_k^{(c)-1}\boldsymbol{e}\right]^{-1}\tag{38}$$

$\boldsymbol{w}_{k-1}$和$\tilde{\boldsymbol{V}}_k^{(w)}$的互协方差阵为

$$\begin{aligned}\tilde{S}_k^{(w)}&=\mathrm{E}\left[\boldsymbol{w}_{k-1}\tilde{\boldsymbol{V}}_k^{(w)\mathrm{T}}\right]\\&=S_k^{(c)}\tilde{\boldsymbol{R}}_k^{(c)-1}\boldsymbol{e}\left[\boldsymbol{e}^{\mathrm{T}}\tilde{\boldsymbol{R}}_k^{(c)-1}\boldsymbol{e}\right]^{-1}\end{aligned}\tag{39}$$

加权观测融合方程可重写为

$$\Delta z_k^{(w)}=\tilde{\boldsymbol{H}}_k^{(w)}\boldsymbol{x}_{k-1}+\tilde{\boldsymbol{V}}_k^{(w)}\tag{40}$$

$$\tilde{\boldsymbol{H}}_k^{(w)}=\tilde{\boldsymbol{H}}_k\tag{41}$$

注4 由文献[2]，上述加权观测融合算法是一种全局最优的融合算法，可得到在相应噪声统计下的最优融合估计。

定理3　带保守上界噪声方差$\boldsymbol{Q}_k$和$\boldsymbol{R}_k^{(i)}$的多传感器加权观测融合不确定增量系统式(1)和式(40)在假设1和假设2下，有带保守和实际滤波误差方差阵各为$\boldsymbol{P}_{k|k}^{(w)}$和$\bar{\boldsymbol{P}}_{k|k}^{(w)}$的实际加权观测融合时变增量Kalman滤波器$\hat{\boldsymbol{x}}_{k|k}^{(w)}$为

$$\hat{\boldsymbol{x}}_{k+1|k}^{(w)}=\boldsymbol{\Phi}_k\hat{x}_{k|k-1}^{(w)}+\boldsymbol{K}_{k+1}^{p(w)}\varepsilon_k^{(w)}\tag{42}$$

$$\boldsymbol{\varepsilon}_k^{(w)} = \Delta\boldsymbol{z}_k^{(w)} - \Delta\hat{\boldsymbol{z}}_{k|k-1}^{(w)} = \Delta\boldsymbol{z}_k^{(w)} - \tilde{\boldsymbol{H}}_k^{(w)}\hat{\boldsymbol{x}}_{k-1|k-1}^{(w)} \tag{43}$$

$$\begin{aligned}\boldsymbol{K}_{k+1}^{p(w)} =& \boldsymbol{\Phi}_k(\boldsymbol{\Phi}_{k-1}\boldsymbol{P}_{k-1|k-1}^{(w)}\tilde{\boldsymbol{H}}_k^{(w)\mathrm{T}} + \boldsymbol{\Gamma}_{k-1}\boldsymbol{S}_{k-1}^{(w)}) \\ & (\tilde{\boldsymbol{H}}_k^{(w)}\boldsymbol{P}_{k-1|k-1}^{(w)}\tilde{\boldsymbol{H}}_k^{(w)\mathrm{T}} + \tilde{\boldsymbol{R}}_k^{(w)})^{-1}\end{aligned} \tag{44}$$

$$\begin{aligned}\boldsymbol{P}_{k+|k}^{(w)} =& \boldsymbol{\Phi}_k\boldsymbol{P}_{k|k-1}^{(w)}\boldsymbol{\Phi}_k^{\mathrm{T}} + \boldsymbol{K}_{k+1}^{p(w)}(\tilde{\boldsymbol{H}}_k^{(w)}\boldsymbol{P}_{k-1|k-1}^{(w)}\tilde{\boldsymbol{H}}_k^{(w)\mathrm{T}} \\ & + \tilde{\boldsymbol{R}}_k^{(w)})^{-1}\boldsymbol{K}_{k+1}^{p(w)\mathrm{T}} + \boldsymbol{\Gamma}_k\boldsymbol{Q}_k\boldsymbol{\Gamma}_k^{\mathrm{T}}\end{aligned} \tag{45}$$

$$\hat{\boldsymbol{x}}_{k+1|k+1}^{(w)} = \hat{\boldsymbol{x}}_{k+1|k}^{(w)} + \boldsymbol{K}_{k+1}^{f(w)}\varepsilon_{k+1}^{(w)} \tag{46}$$

$$\begin{aligned}\boldsymbol{K}_{k+1}^{f(w)} =& (\boldsymbol{\Phi}_k\boldsymbol{P}_{k|k}^{(w)}\tilde{\boldsymbol{H}}_{k+1}^{(w)\mathrm{T}} + \boldsymbol{\Gamma}_k\boldsymbol{S}_k^{(w)}) \\ & \cdot(\tilde{\boldsymbol{H}}_k^{(w)}\boldsymbol{P}_{k|k}^{(w)}\tilde{\boldsymbol{H}}_k^{(w)\mathrm{T}} + \tilde{\boldsymbol{R}}_k^{(w)})^{-1}\end{aligned} \tag{47}$$

$$\begin{aligned}\boldsymbol{P}_{k+1|k+1}^{(w)} =& \boldsymbol{P}_{k+1|k}^{(w)} + \boldsymbol{K}_{k+1}^{f(w)}\cdot(\tilde{\boldsymbol{H}}_k^{(w)}\boldsymbol{P}_{k|k}^{(w)}\tilde{\boldsymbol{H}}_{k+1}^{(w)\mathrm{T}} \\ & + \tilde{\boldsymbol{R}}_{k+1}^{(w)})\boldsymbol{K}_{k+1}^{f(w)\mathrm{T}}\end{aligned} \tag{48}$$

带初值$\hat{\boldsymbol{x}}_{0|0}^{(w)} = \mu$，$\boldsymbol{P}_{0|0}^{(w)} = P_{0|0}$和$\bar{\boldsymbol{P}}_{0|0}^{(w)} = \bar{P}_{0|0}$，其中$\Delta\boldsymbol{z}_k^{(w)}$为带实际局部观测$\Delta\boldsymbol{z}_k^{(i)}$的实际融合观测式(35)。代入实际噪声方差易得$\bar{\boldsymbol{P}}_{k+|k}^{(w)}$和$\bar{\boldsymbol{P}}_{k+1|k+1}^{(w)}$。

证明　由文献[14]，基于加权观测融合系统模型式(1)和式(40)，应用增量Kalman滤波算法，易得定理3。

定理4　多传感器不确定系统式(1)和式(2)在假设1和假设2下，对所有容许的满足式(3)的$\bar{\boldsymbol{Q}}_k$，$\bar{\boldsymbol{R}}_k^{(i)}$和满足式(5)的初值$\bar{\boldsymbol{P}}_{0|0}$，实际加权观测融合时变增量Kalman滤波器式(42)—式(48)是鲁棒的，即

$$\bar{\boldsymbol{P}}_{k|k}^{(w)} \le \boldsymbol{P}_{k|k}^{(w)} \tag{49}$$

且$\boldsymbol{P}_{k|k}^{(w)}$是$\bar{\boldsymbol{P}}_{k|k}^{(w)}$的最小上界。

证明　对于加权观测融合系统式(1)和式(40)，由式(3)、式(37)和式(38)得$\bar{\boldsymbol{Q}}_k \le \boldsymbol{Q}_k$，且有$\bar{\boldsymbol{R}}_k^{(w)} \le \boldsymbol{R}_k^{(w)}$。类似定理2的证明可得式(49)成立。　证毕

注5 类似注3单传感器的情形，定理4同样可以根据Kalman滤波器的性质，基于Lyapunov方程证明所提出的加权观测融合增量滤波器在式(49)意义上的鲁棒性。

5　实验模型及结果分析

设线性离散增量系统为

$$x_k = 0.2x_{k-1} + w_k \tag{50}$$

$$\Delta z_k^i = x_k - x_{k-1} + V_k^i \tag{51}$$

其中，w_k和V_k^i是零均值、未知实际方差分别为$\bar{Q}$和$\bar{R}^{(i)}$的不相关高斯白噪声。在仿真中，取$Q = 0.1$，$R^1 = 1$，$R^2 = 2$，$R^3 = 3$，$\bar{Q} = 0.08$，$\bar{R}^1 = 0.8$，$\bar{R}^2 = 1.5$，$\bar{R}^3 = 2.2$，初值$x_0 = 0$，$\mu = 0$，$P_{0|0}^{(i)} = 1.1$，$\bar{P}_{0|0}^{(i)} = 1$。量测系统误差$a_k^i = 3$是未知的。

分别应用文献[1]的经典Kalman滤波算法、文献[14]的实际精确增量滤波算法和本文定理1和定理3所提出的鲁棒滤波算法进行了系统的状态估计。仿真结果如图1—图4和表1所示。图1—图4给出了ρ=100Monte-Carlo仿真实验的鲁棒增量Kalman滤波的均方误差曲线(MSE)，在时刻k的局部和融合鲁棒增量Kalman滤波器$\hat{x}_{k|k}^{(\theta)}$的MSE定义为

$$\mathrm{MSE}_k^{(\theta)} = \frac{1}{\rho}\sum_{j=1}^{\rho}(x_k^j - \hat{x}_{k|k}^{(\theta)j})^{\mathrm{T}}(x_k^j - \hat{x}_{k|k}^{(\theta)j}) \tag{52}$$

其中，x_k^j或$\hat{x}_{k|k}^{(\theta)j}$分别表示$x_k$和$\hat{x}_{k|k}^{(\theta)}$的第$j$个实现。图1—图3分别针对3个局部传感器得到的局部经典

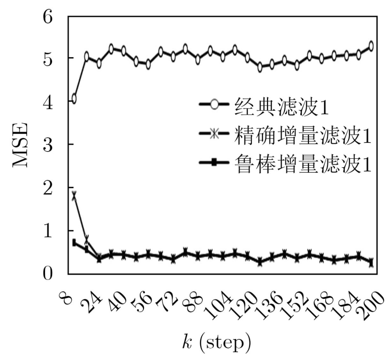

图 1 局部传感器1的经典滤波器、精确增量滤波器和鲁棒增量滤波器均方误差比较

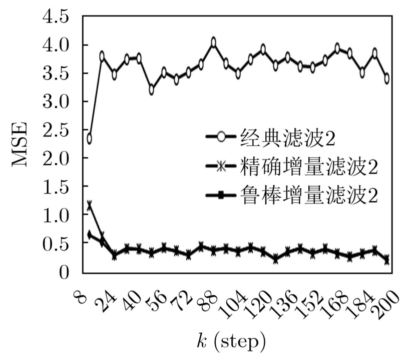

图 2 局部传感器2的经典滤波器、精确增量滤波器和鲁棒增量滤波器均方误差比较

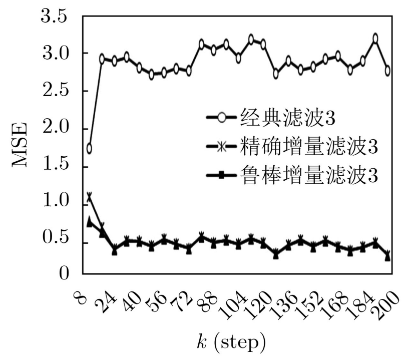

图 3 局部传感器3的经典滤波器、精确增量滤波器和鲁棒增量滤波器均方误差比较

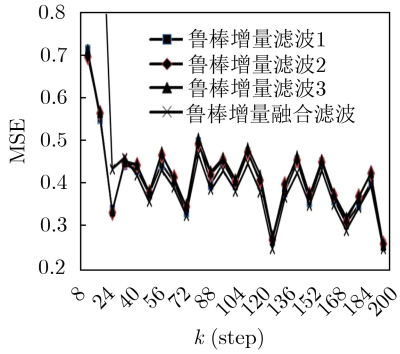

图 4 局部和加权融合鲁棒增量Kalman滤波器的均方误差比较

表 1　局部和加权融合鲁棒增量Kalman滤波器在时刻*k*=200时的均方误差值比较

传感器1	传感器2	传感器3	融合器
0.2593	0.2610	0.2597	0.2490

Kalman滤波器、实际精确增量Kalman滤波器和鲁棒增量Kalman滤波器进行了MSE曲线比较。可见本文所提出的鲁棒增量Kalman滤波器的估计精度远远优于文献[1]的经典Kalman滤波器的估计精度，且非常接近文献[14]的实际精确增量Kalman的估计精度。图4给出了局部和加权观测融合鲁棒增量Kalman滤波器的MSE比较曲线。可见融合算法的引入可以提高多传感器系统的状态估计的精度。表2给出了时刻k=200时局部和加权观测融合鲁棒增量Kalman滤波器的MSE值比较。从数值上比较了局部和加权观测融合鲁棒增量Kalman滤波器的估计精度。可见所提出的加权融合鲁棒增量Kalman滤波算法可有效提高带未知量测误差和未知噪声方差的多传感器不确定系统的状态估计精度，方法有效可行。

6　结束语

对于带未知量测系统误差和未知噪声方差的多传感器不确定系统，本文首先提出了一种基于增量方程的鲁棒增量Kalman滤波算法；进而提出一种最优加权观测融合鲁棒增量Kalman滤波算法，可有效解决带未知量测系统误差和未知噪声方差的多传感器不确定系统的状态估计问题。仿真说明了所提出算法的有效性。

参 考 文 献

[1] KALMAN R E. A new approach to linear filtering and prediction problems[J]. *Journal of Fluids Engineering*, 1960, 82(1): 35–45. doi: 10.1115/1.3662552.

[2] 邓自立, 齐文娟, 张鹏. 鲁棒整合卡尔曼滤波理论及应用[M]. 哈尔滨: 哈尔滨工业大学出版社, 2016: 4.
DENG Zili, QI Wenjuan, and ZHANG Peng. Robust Fusion Kalman Filtering Theory with Applications[M]. Harbin: Harbin Institute of Technology Press, 2016: 4.

[3] 杨峰, 郑丽涛, 王家琦, 等. 双层无迹卡尔曼滤波[J]. 自动化学报, 2019, 45(7): 1386–1391. doi: 10.16383/j.aas.c180349.
YANG Feng, ZHENG Litao, WANG Jiaqi, *et al*. Double layer unscented Kalman filter[J]. *Acta Automatica Sinica*, 2019, 45(7): 1386–1391. doi: 10.16383/j.aas.c180349.

[4] 张宏伟, 谢维信. 平滑约束无迹卡尔曼滤波器[J]. 信号处理, 2019, 35(3): 466–471. doi: 10.16798/j.issn.1003-0530.2019.03.019.
ZHANG Hongwei and XIE Weixin. Smoothly constrained unscented Kalman filter[J]. *Journal of Signal Processing*, 2019, 35(3): 466–471. doi: 10.16798/j.issn.1003-0530.2019.03.019.

[5] 耿友林, 解成博, 尹川, 等. 基于卡尔曼滤波的接收信号强度指示差值定位算法[J]. 电子与信息学报, 2019, 41(2): 455–461. doi: 10.11999/JEIT180268.
GENG Youlin, XIE Chengbo, YI Chuan, *et al*. Received signal strength indication difference location algorithm based on Kalman filter[J]. *Journal of Electronics & Information Technology*, 2019, 41(2): 455–461. doi: 10.11999/JEIT180268.

[6] 王少帅, 李登峰. 基于无迹卡尔曼滤波的路面附着系数估计[J]. 电子设计工程, 2020, 28(1): 27–31. doi: 10.14022/j.issn1674-6236.2020.01.007.
WANG Shaoshuai and LI Dengfeng. Road adhesion coefficient estimation based on unscented Kalman filter[J]. *Electronic Design Engineering*, 2020, 28(1): 27–31. doi: 10.14022/j.issn1674-6236.2020.01.007.

[7] 沈连丰, 张瑞, 朱亚萍, 等. 面向自动驾驶的车辆精确实时定位算法[J]. 电子与信息学报, 2020, 42(1): 28–35. doi: 10.11999/JEIT190610.
SHEN Lianfeng, ZHANG Rui, ZHU Yaping, *et al*. High-precision and real-time localization algorithm for automatic driving vehicles[J]. *Journal of Electronics & Information Technology*, 2020, 42(1): 28–35. doi: 10.11999/JEIT190610.

[8] SUN Xiaojun, GAO Yuan, DENG Zili, *et al*. Multi-model information fusion Kalman filtering and white noise deconvolution[J]. *Information Fusion*, 2010, 11(2): 163–173. doi: 10.1016/j.inffus.2009.06.004.

[9] 刘利生, 吴斌, 杨萍. 航天器精确定轨与自校准技术[M]. 北京: 国防工业出版社, 2005: 9.
LIU Lisheng, WU Bin, and YANG Ping. Orbit Precision Determination & Self-Calibration Technique of Spacecraft[M]. Beijing: National Defense Industry Press, 2005: 9.

[10] 傅惠民, 娄泰山, 吴云章. 欠观测条件下的扩展增量Kalman滤波方法[J]. 航空动力学报, 2012, 27(4): 777–781. doi: 10.13224/j.cnki.jasp.2012.04.004.

FU Huimin, LOU Taishan, and WU Yunzhang. Extended incremental Kalman filter method under poor observation condition[J]. *Journal of Aerospace Power*, 2012, 27(4): 777–781. doi: 10.13224/j.cnki.jasp.2012.04.004.

[11] 傅惠民, 娄泰山, 吴云章. 增量粒子滤波方法[J]. 航空动力学报, 2013, 28(6): 1201–1207. doi: 10.13224/j.cnki.jasp.2013.06.005.

FU Huimin, LOU Taishan, and WU Yunzhang. Incremental particle filter method[J]. *Journal of Aerospace Power*, 2013, 28(6): 1201–1207. doi: 10.13224/j.cnki.jasp.2013.06.005.

[12] 傅惠民, 吴云章, 娄泰山. 欠观测条件下的增量Kalman滤波方法[J]. 机械强度, 2012, 34(1): 43–47. doi: 10.16579/j.issn.1001.9669.2012.01.014.

FU Huimin, WU Yunzhang, and LOU Taishan. Incremental Kalman filter method under poor observation condition[J]. *Journal of Mechanical Strength*, 2012, 34(1): 43–47. doi: 10.16579/j.issn.1001.9669.2012.01.014.

[13] 孙小君, 周晗, 闫广明. 基于新息的自适应增量Kalman滤波器[J]. 电子与信息学报, 2020, 42(9): 2223–2230. doi: 10.11999/JEIT190493.

SUN Xiaojun, ZHOU Han, and YAN Guangming. Adaptive incremental Kalman filter based on innovation[J]. *Journal of Electronics & Information Technology*, 2020, 42(9): 2223–2230. doi: 10.11999/JEIT190493.

[14] SUN Xiaojun and YAN Guangming. Multi-sensor optimal weighted fusion incremental Kalman smoother[J]. *Journal of Systems Engineering and Electronics*, 2018, 29(2): 262–268. doi: 10.21629/JSEE.2018.02.06.

[15] 蔡博, 高宏力, 宋兴国, 等. 基于改进增量卡尔曼滤波算法的UWB室内定位研究[J]. 机械设计与制造, 2020(2): 22–25. doi: 10.3969/j.issn.1001-3997.2020.02.006.

CAI Bo, GAO Hongli, SONG Xingguo, *et al*. Research of UWB indoor location based on improved incremental Kalman filter algorithm[J]. *Machinery Design & Manufacture*, 2020(2): 22–25. doi: 10.3969/j.issn.1001-3997.2020.02.006.

[16] 伍锡锈. 基于增量Kalman滤波的GPS多路径效应系统误差研究[J]. 测绘工程, 2012, 21(6): 35–37. doi: 10.3969/j.issn.1006-7949.2012.06.009.

WU Xixiu. GPS multipath effect systematic error research based on incremental Kalman filter[J]. *Engineering of Surveying and Mapping*, 2012, 21(6): 35–37. doi: 10.3969/j.issn.1006-7949.2012.06.009.

[17] 肖曦, 王伟华, 吕志鹏. 一种基于增量式卡尔曼滤波器的PMSM转速滤波算法[J]. 电机与控制学报, 2014, 18(10): 104–111. doi: 10.3969/j.issn.1007-449X.2014.10.016.

XIAO Xi, WANG Weihua, and LÜ Zhipeng. Filtering algorithm of speed for PMSM based on incremental Kalman filter[J]. *Electric Machines and Control*, 2014, 18(10): 104–111. doi: 10.3969/j.issn.1007-449X.2014.10.016.

[18] LEWIS F L, XIE Lihua, and POPA Dan. Optimal and Robust Estimation[M]. 2nd ed. Boca Raton: CRC Press, 2008.

[19] QU Xiaomei and ZHOU Jie. The optimal robust finite-horizon Kalman filtering for multiple sensors with different stochastic failure rates[J]. *Applied Mathematics Letters*, 2013, 26(1): 80–86. doi: 10.1016/j.aml.2012.03.036.

[20] ZHU Xing, SOH Y C, and XIE Lihua. Design and analysis of discrete-time robust Kalman filters[J]. *Automatica*, 2002, 38(6): 1069–1077. doi: 10.1016/S0005-1098(01)00298-9.

[21] XI Hongsheng. The guaranteed estimation performance filter for discrete-time descriptor systems with uncertain noise[J]. *International Journal of Systems Science*, 1997, 28(1): 113–121. doi: 10.1080/00207729708929368.

[22] ZHAO Dong, DING S X, KARIMI H R, *et al*. On robust Kalman filter for two-dimensional uncertain linear discrete time-varying systems: A least squares method[J]. *Automatica*, 2019, 99: 203–212. doi: 10.1016/j.automatica.2018.10.029.

[23] DONG Zhe and YOU Zheng. Finite-horizon robust Kalman filtering for uncertain discrete time-varying systems with uncertain-covariance white noises[J]. *IEEE Signal Processing Letters*, 2006, 13(8): 493–496. doi: 10.1109/LSP.2006.873148.

[24] 傅惠民, 吴琼. 线性独立增量过程分析方法[J]. 航空动力学报, 2010, 25(4): 930–935.

FU Huimin and WU Qiong. Analysis method for linear process with independent increments[J]. *Journal of Aerospace Power*, 2010, 25(4): 930–935.

孙小君：女，1980年生，副教授，研究方向为多传感器信息融合、状态估计、信号处理.

周　晗：男，1993年生，硕士生，研究方向为多传感器信息融合、系统辨识.

沈海滨：男，1994年生，硕士生，研究方向为多传感器信息融合、系统辨识.

闫广明：男，1979年生，讲师，研究方向为多传感器信息融合、状态估计.

责任编辑：马秀强